



## Removal of ruthenium from high-level radioactive liquid waste generated during reprocessing of spent fuel

Khushboo Singh<sup>a\*</sup>, N.L. Sonar<sup>a</sup>, T.P. Valsala<sup>a</sup>, Y. Kulkarni<sup>a</sup>, Tessy Vincent<sup>b</sup>, Amar Kumar<sup>b</sup>

<sup>a</sup>Waste Immobilization Plant, Nuclear Recycle Board, Bhabha Atomic Research Centre, Tarapur 401502, India  
Email: sona.khushboo705@gmail.com

<sup>b</sup>Process Development Division, Nuclear Recycle Group, Bhabha Atomic Research Centre, Trombay, Mumbai 400085, India

Received 16 April 2012; Accepted 2 September 2013

---

### ABSTRACT

Radio-ruthenium (Ru) due to its existence in the form of complexes with varied oxidation state, larger fission yield and relatively long half life is an extremely troublesome nuclide during reprocessing and subsequent waste management. In the process of the concentration of high-level waste (HLW), containing many nitrates of fission products and nitric acid, Ru is oxidised to volatile tetroxide RuO<sub>4</sub>, which is reduced to its dioxide (RuO<sub>2</sub>) at the inner surface of the equipment and is deposited there. As a result, the radiation dose of the plant equipments keeps increasing. A process was developed for the separation of Ru from HLW stream by volatilisation using KMnO<sub>4</sub> (potassium permanganate) and O<sub>3</sub> (ozone) as oxidising agent and its subsequent trapping on adsorbent material polyether ether ketone pellets. Various parameters like acidity, Ru concentration, temperature, time period of reaction and type of adsorbent were studied. The sorption behaviour was examined with various isotherms like Langmuir, Freundlich and Dubinin–Raduskevich isotherms. Thermodynamics parameters were also evaluated. The results indicated that maximum volatilisation of Ru occurred in the case of KMnO<sub>4</sub> (98%) as compared to O<sub>3</sub> (53%) at low acid concentration (2 M).

*Keywords:* Ruthenium (Ru); Simulated high-level liquid waste (SHLLW); Polyether ether ketone (PEEK)

---

### 1. Introduction

PUREX solvent extraction process is being conventionally employed for reprocessing of spent fuel. It mainly involves co-decontamination cum partitioning cycle followed by purification cycles for

recovery of valuable U and Pu. Most of the radioactivity associated with the spent fuel remains in the raffinate stream of the extraction column of the co-decontamination cum partitioning cycle. This waste stream is further concentrated and termed as high-level liquid waste (HLLW). High-level waste (HLW) in acidic condition is stored in stainless steel tanks.

\*Corresponding author.

Presented at the DAE—BRNS Biennial Symposium on Emerging Trends in Separation Science and Technology (SESTEC 2012) Mumbai, India, 27 February–1 March 2012

Vitrification process based on sodium borosilicate glass matrix [1] has been accepted and adopted for immobilisation of HLW.

During vitrification process, in the presence of nitric acid, radio-ruthenium (Ru) is oxidised to volatile tetroxide and escapes to the vapour phase. Its subsequent decomposition to RuO<sub>2</sub> leads to plating out on cooler surfaces in the off gas lines resulting in hot spots. The problems associated with Ru volatilisation could be aggravated in case of short cooled fuel having higher Ru activity. To some extent, this Ru reports in subsequent aqueous waste stream like intermediate and low level waste.

Radio-Ru is hazardous due to its chemical and radio toxicity. The occurrence of the relatively long-lived isotopes of Ru, like <sup>103</sup>Ru and <sup>106</sup>Ru, amongst the fission products, forms tetravalent nitrosyl-Ru complexes in which the ligands are nitrate, nitro, hydroxo and aquo groups. Ru is analogous to the transition elements cobalt, iron and nickel in its formation of numerous coordination complexes with the ligands like O, Cl, NO, NO<sub>2</sub>, NO<sub>3</sub><sup>-</sup>, etc. [2]. A series of nitroaquo nitrosyl ruthenium complexes were identified with general formula [RuNO(NO<sub>3</sub>)<sub>x</sub>(NO<sub>2</sub>)<sub>y</sub>(OH)<sub>z</sub>(H<sub>2</sub>O)<sub>5-x-y-z</sub>]<sup>3-x-y-z</sup> [3]. In aqueous solution, Ru may exist in anionic or cationic form depending on the type of ligand it is associated with.

The oxides of Ru that are encountered most often in radiochemistry are RuO<sub>4</sub> and RuO<sub>2</sub>. Ru volatilises as RuO<sub>4</sub> in the temperature range of 45–110°C. RuO<sub>2</sub> in contrast to RuO<sub>4</sub>, behaves similarly to manganese dioxide; the refractory form is obtained by thermal destruction of Ru. The usual radiochemical form of the dioxide is the hydrous oxide RuO(OH)<sub>2</sub>, which is readily soluble in warm hydrochloric acid but is less soluble in nitric acid and in sulphuric acid [4].

Various researchers have made use of activated charcoal as sorbent for sorption of Ru from nitric acid media as a function of Ru ions concentration and temperature [5].

A classical filtration mechanism by making use of silica gel as an adsorbent for removal of Ru in aerosol form is reported. However, only a minute fraction of the aerosol form of Ru is trapped [6]. Screening of silver nanoparticles containing carbonised yeast cells is also tried for adsorption of Ru by Selvakumar et al. [7].

Adsorption of Ru on amorphous Fe(OH)<sub>3</sub>, α-Fe<sub>2</sub>O<sub>3</sub> and Fe<sub>3</sub>O<sub>4</sub> have been measured as a function of the pH and the time of aging. The results indicated that the complexation of Ru ions, with organic ligands, strongly suppresses the adsorption of Ru on Fe<sub>3</sub>O<sub>4</sub> [6].

Perchloric acid treated iron oxide coated siliceous brick granules (PERCOSIB) were installed to adsorb

Ru from the off-gases from Joule Melter at Tarapur. However, the sorbent PERCOSIB could not efficiently adsorb Ru. To overcome these problems, present study was focused for the development of a process for the separation of Ru from HLLW stream by volatilisation with suitable oxidising agent and its subsequent trapping using suitable adsorbents. Oxidants like KMnO<sub>4</sub> (potassium permanganate), K<sub>2</sub>S<sub>2</sub>O<sub>8</sub> (potassium persulphate) have been selected. Use of ozone, as the powerful oxidising agent, is also tried as it does not alter the composition of HLLW. Materials like silicon and polyether ether ketone (PEEK) having better radiation stability was tried for adsorbing ruthenium tetroxide (RuO<sub>4</sub>).

## 2. Materials

For the volatilisation cum adsorption experiments, different oxidising agents viz, KMnO<sub>4</sub> (MERCK, product No. 119246; purity 99.8%), ozone (analytical grade) and K<sub>2</sub>S<sub>2</sub>O<sub>8</sub> (MERCK, product No. 119259; purity 99.4%) and adsorbents like PEEK pellets (M/s Polyester Polymer Industries, India porosity 55%, specific gravity 1320 kg/m<sup>3</sup> at 25°C) and silicon tubes (M/s M. K. Silicone Products Pvt. Ltd., India porosity 32%, specific gravity 1,150 kg/m<sup>3</sup> at 25°C) were used.

## 3. Experimental

### 3.1. Preparation of simulated HLW

Simulated HLLW was prepared with all the components as listed in Table 1. The salts of the components used were of AR grade. While preparing simulated high-level liquid waste (SHLLW), Ru was not added. It was mixed prior to experiments since studies were conducted by varying the Ru concentration from 100 to 500 ppm. Ru was added in SHLLW in the form Ru-nitrate.

### 3.2. Ru volatilisation explanation

All the experiments were performed in 150 mL batch size. The experiments were performed using the set-up shown in Fig. 1. The set-up consist of reaction vessel of 1 L capacity and an adsorption column with the provision of jacket cooling. The mixture in the reaction vessel was heated by a mantle heater at constant heat flux to maintain continuous boiling under reflux condition. Air was used as carrier gas at a flow rate of 2 lph. The gases coming out of the adsorbing column were passed through a scrubber bottle

Table 1  
Typical simulated waste composition

Element	Conc. (g/L)	Salt	Salt conc. (g/L)	Salt conc. (g/5L)
Fe	0.6	Fe(NO <sub>3</sub> ) <sub>3</sub> ·9H <sub>2</sub> O	4.3404	21.702
Na	4	NaNO <sub>3</sub>	14.7824	73.912
Ni	0.3	Ni(NO <sub>3</sub> ) <sub>2</sub> ·6H <sub>2</sub> O	1.48575	7.42875
K	0.3	KNO <sub>3</sub>	0.7758	3.88
Cr	0.22	CrO <sub>3</sub>	0.42306	2.1153
Mn	0.72	Mn(NO <sub>3</sub> ) <sub>2</sub> ·6H <sub>2</sub> O	3.760344	18.80172
Sr	0.06	Sr(NO <sub>3</sub> ) <sub>2</sub>	0.144912	0.72456
Zr	0.006	Zr(NO <sub>3</sub> ) <sub>4</sub> ·5H <sub>2</sub> O	0.028232	0.14116
Mo	0.195	MoO <sub>3</sub>	0.2925	1.4625
Te	0.036	TeO <sub>2</sub>	0.045	0.225
Ba	0.375	Ba(NO <sub>3</sub> ) <sub>2</sub>	0.713625	3.568125
La	0.18	La(NO <sub>3</sub> ) <sub>3</sub> ·6H <sub>2</sub> O	0.56115	2.80575
Ce	0.06	Ce(NO <sub>3</sub> ) <sub>3</sub> ·6H <sub>2</sub> O	0.185925	0.929625
Nd	0.12	Nd(NO <sub>3</sub> ) <sub>3</sub> ·5H <sub>2</sub> O	0.349728	1.74864
Y	0.06	Y(NO <sub>3</sub> ) <sub>3</sub> ·6H <sub>2</sub> O	0.25825	1.292625
Al	0.255	Al(NO <sub>3</sub> ) <sub>3</sub> ·9H <sub>2</sub> O	3.54603	17.73015
Cs	0.315	CsNO <sub>3</sub>	0.46179	2.32395



Fig. 1. Experimental set-up for volatilisation cum adsorption. Ru concentration 126–500 ppm, nitric acid concentration 2–6 M, temperature 60–80°C, adsorbent PEEK, silicone tubes, oxidant KMnO<sub>4</sub>, O<sub>3</sub>, K<sub>2</sub>S<sub>2</sub>O<sub>8</sub>.

containing 1 M NaOH solution. Since the experimentation involves radio-tracer, experimental set-up was installed in a fume hood. During the course of the experiments to understand the volatilisation/oxidation behaviour of Ru, periodic samples were collected from reaction vessel as well as scrubber and analysed for Ru by multichannel analyser using HPGe as detector.

Various sets of experiments were conducted by changing various parameters like type of oxidant, type of adsorbent, time period, temperature, concentration

of nitric acid as well as Ru. <sup>106</sup>Ru as tracer was added to the SHLLW so as to enable radioactive ease of measurement. The oxidants were added in the ratio of oxidising agent to SHLLW as 1.5:150 (wt./volume). Ozone was also tried as an oxidising agent. Ozone was fed to the reaction vessel at the rate of 1–2 lph using an ozone generator (make: M/s. Universal Ozone System, India). The adsorbing column was filled with suitable quantity of PEEK or silicone material. PEEK was available in the rod form (1 m length × 8 mm diameter). It was cut in the form of pellets and used as packing in adsorption column. Silicone tubes were in cylindrical shape. The adsorbing column was installed just above the reaction vessel.

#### 4. Results and discussion

The Ru concentration in the typical HLW was in the range of 100–150 ppm, hence during the experimental study the Ru concentration was varied from 100 to 500 ppm. The nitric acid concentration was also varied from 2 to 6 M. The data obtained during temperature study was used to derive thermodynamic parameters and the data obtained by varying Ru concentration was used to understand the sorption behaviour by applying various sorption isotherms. All the set of experiments were performed in triplicate and the average data were taken for evaluation. The percentage of Ru volatilisation is calculated from the given equation.

$$\% \text{ Ru volatilised} = (1 - (A_t/A_o)) \times 100$$

where  $A_t$  is concentration of Ru left in the reaction vessel at time  $t$  and  $A_o$  is the initial concentration of Ru present in the solution. As a first approximation, it has been assumed that the volatilisation of Ru obeys the first-order rate equation [8].

#### 4.1. Selection of adsorbent

Initial study was conducted to examine the adsorption behaviour of Ru on the adsorbing material PEEK and silicone tubes using SHLLW with 4 M nitric acid and  $\text{KMnO}_4$  as oxidising agent. Ru concentration was taken as 126 ppm.

The amount of Ru adsorbed on silicone was observed to be low as compared to PEEK. Performance of adsorption behaviour is compared in Fig. 2.

In the case of PEEK as adsorbent, the scrub solution has shown no activity of Ru, indicating that all escaped Ru got adsorbed on PEEK. However, in the case of the silicone adsorbent, some activity was reported in the scrub solution. This may be due to more porosity of PEEK pellets as compared to the silicone tubes. Based on these observations, further studies were conducted using PEEK as sorbent.

#### 4.2. Effect of oxidising agent

Experiments were conducted using ozone,  $\text{KMnO}_4$ ,  $\text{K}_2\text{S}_2\text{O}_8$  as an oxidant with SHLLW in 4 M nitric acid after charging the column with PEEK pellets. Reaction

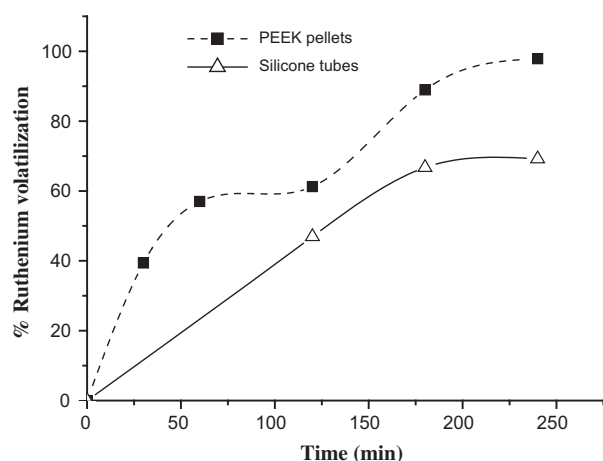


Fig. 2. Sorption behaviour of Ru on PEEK and silicone material oxidant:  $\text{KMnO}_4$ . Ru concentration 126 ppm, nitric acid concentration 4 M, temperature 80°C, adsorbent PEEK, silicone tubes, oxidant  $\text{KMnO}_4$ .

temperature was kept at 80°C and Ru concentration was also kept constant 126 ppm in simulated waste. For comparing their performance, one experiment was done with SHLLW of 4 M free acidity without use of any oxidant.

The highest per cent volatilisation was observed in the case of  $\text{KMnO}_4$ . (Fig. 3). This could be due to the higher electrode potential of  $\text{KMnO}_4$  as compared to ozone and  $\text{K}_2\text{S}_2\text{O}_8$ . However, in the case of SHLLW solution without adding any oxidising agent, only 10% volatilisation was obtained. Lower volatilisation in the case of ozone may be due to the fact that  $\text{O}_3$  is gas and it has less residence time in the reaction vessel. With these observations, the rest of the experiments were conducted using only two oxidants  $\text{KMnO}_4$  and  $\text{O}_3$ .

#### 4.3. Effect of acid concentration

Experiments were conducted for 2 h duration at 80°C using SHLLW having acidity varying from 2 to 6 M and Ru concentration was maintained at 126 ppm. The volatilisation behaviour of Ru as a function of acid concentration is shown in Fig. 4 for  $\text{KMnO}_4$  and  $\text{O}_3$ .

The results indicate that the maximum volatilisation of Ru ions occurred at a low acid concentration (2 M). It is in concurrence with the reported literature [9]. At a low acid concentration, the Ru ions ( $\text{Ru}^{3+}$ ) from vapours get adsorbed onto the surface of PEEK pellets as such, thereby leading to high adsorption. The decrease in the volatilisation of Ru ions with the increase in acidity is because of competitive reaction

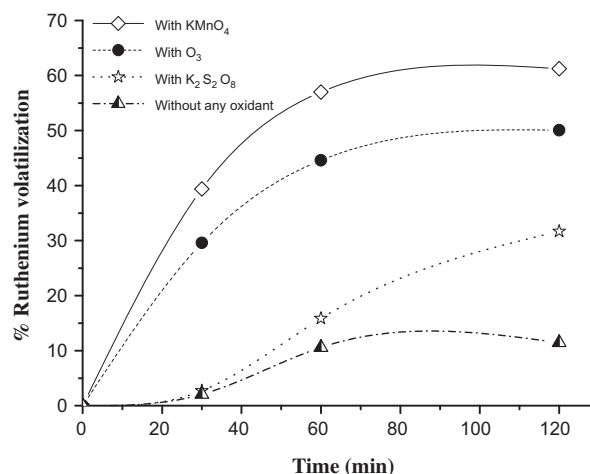


Fig. 3. Influence of different oxidising agent on Ru volatilisation from simulated waste in 4 M nitric acid concentration at 80°C. Ru concentration 126 ppm, adsorbent PEEK, oxidants  $\text{KMnO}_4$ ,  $\text{O}_3$ ,  $\text{K}_2\text{S}_2\text{O}_8$ .

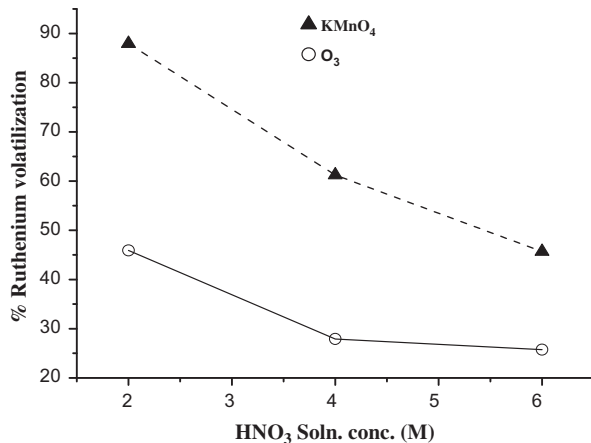


Fig. 4. Influence of nitric acid solution concentration on Ru volatilisation (KMnO<sub>4</sub> and O<sub>3</sub>) at 80°C. Ru concentration 126 ppm, nitric acid concentration 2–6 M, adsorbent PEEK, oxidants KMnO<sub>4</sub>, O<sub>3</sub>.

between excess of H<sup>+</sup> ions in the medium and positively charged species, Ru<sup>3+</sup> present in the solution [10]. The extent of volatilisation is decreased with the increase in acid concentration. This behaviour is the same for both KMnO<sub>4</sub> and O<sub>3</sub>.

#### 4.4. Effect of temperature

Experiments were performed with SHLLW having 4 M acidity and 126 ppm of Ru concentration using oxidising agents KMnO<sub>4</sub> and O<sub>3</sub>. The temperature was varied from 60 to 80°C. The extent of Ru volatilisation is shown in Fig. 5 for KMnO<sub>4</sub> and O<sub>3</sub>. As seen

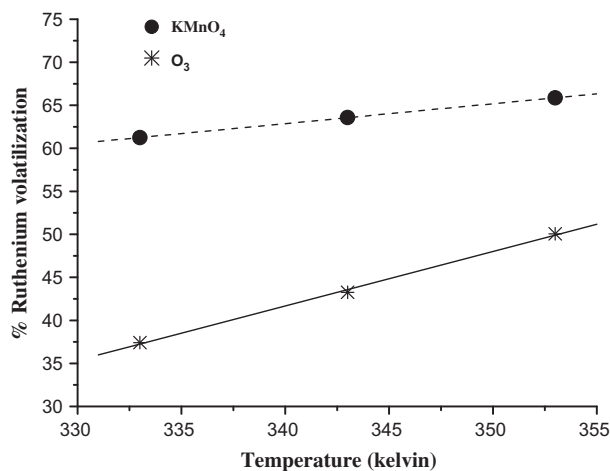


Fig. 5. Influence of temperature on Ru volatilisation (Ru concentration 126 ppm, adsorbent: PEEK, SHLLW with 4 M nitric acid concentration, oxidants KMnO<sub>4</sub> and O<sub>3</sub>) at 80°C, R = 0.999 (KMnO<sub>4</sub>), R = 0.999 (O<sub>3</sub>).

from the figure, per cent volatilisation increases with the increase in temperature.

#### 4.5. Influence of the Ru concentration

To investigate the behaviour of Ru concentration on its volatility, experiments were performed by varying the concentration of Ru from 126, 300, 400 and 500 ppm from 4 M SHLLW using KMnO<sub>4</sub> and O<sub>3</sub> as oxidising agent on PEEK pellets.

Graph is plotted between amounts of Ru ions adsorbed (mg/g) and Ru concentration left in the solution at equilibrium.

Fig. 6 depicts the adsorption isotherm of Ru ions on PEEK pellets from simulated waste with 4 M nitric acid concentration. The figure shows that the adsorption of Ru ions on PEEK pellets increases with the increase in the concentration of Ru ions. This shows that with increase in concentration in solution, the vapour phase concentration of Ru is also increasing. The observed increase is quite obvious as on increasing the concentration of Ru ions, greater number of metal ions arrives at the interface and thus gets adsorbed [9].

#### 4.6. Volatilisation of Ru to RuO<sub>4</sub>

Volatilisation of Ru from nitric acid solutions has been observed in the dissolution of spent nuclear fuel and in the treatment of HLW [11]. Higher nitric acid concentration, higher temperature and prolonged hold-up time of the solution enhance the volatilisation of Ru [12]. The following reactions were proposed for oxidation of Ru by nitrate [8]:

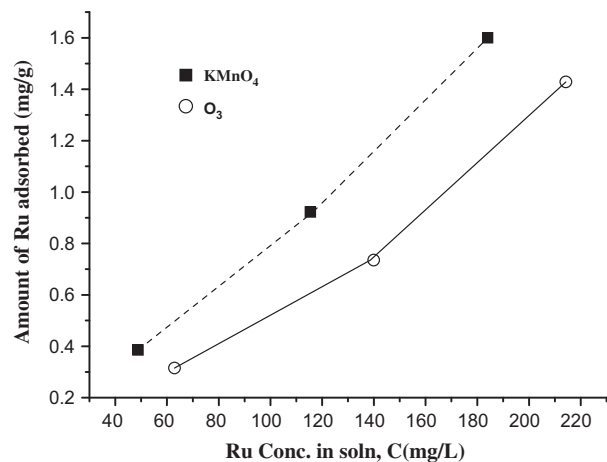
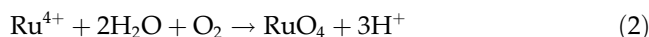


Fig. 6. Influence of Ru ions concentration on its volatilisation (Ru concentration 126–500 ppm, adsorbent PEEK, SHLLW with 4 M nitric acid concentration, oxidants KMnO<sub>4</sub> and O<sub>3</sub>) at 80°C.



After an induction period, the volatilisation of ruthenium occurred. The volatilisation of Ru from boiling nitric acid depends on both the concentration of nitric acid and Ru present in the solution. The percentage of Ru volatilised at a certain time is calculated as follows:

$$\alpha = (A_t/A_o) \quad (4)$$

$$\% \text{ Ru volatilised} = (1 - (A_t/A_o)) \times 100 \quad (5)$$

where  $A_t$  is concentration of Ru left in the reaction vessel at time  $t$  and  $A_o$  is the initial concentration of Ru present in the solution. As a first approximation, it has been assumed that the volatilisation of Ru obeys the first-order rate equation [8]:

$$d\alpha/dt = k(1 - \alpha)$$

where  $k$  is the rate constant. Thus, the relation between  $\alpha$  and  $t$  is given as:

$$-\ln(1 - \alpha) = kt \quad (6)$$

where  $t$  is the boiling duration of the solution. Accordingly, from the plot of  $-\ln(1 - \alpha)$  against  $t$ , the rate constant  $k$  is obtained. The value,  $-\ln(1 - \alpha)$  increases almost linearly with boiling time as expected from Eq. (6).

The volatilisation behaviour of Ru as a function of boiling time for various acidities is shown in Fig. 7 for  $\text{KMnO}_4$  and Fig. 8 for  $\text{O}_3$ . The value,  $-\ln(1 - \alpha)$  increases almost linearly with boiling time as expected from Eq. (6). Experiments were conducted to examine the Ru volatilisation by using two different oxidising agents  $\text{KMnO}_4$  and  $\text{O}_3$ . The volatilisation rates are tabulated in Table 2 for various acidities.

The results in Table 2 indicate that maximum volatilisation of Ru ions occurred in the case of  $\text{KMnO}_4$  as compared to ozone which has been seen from the rate constant values for a different nitric acid concentration.

The Ru volatilisation rate is found to be higher in the case of  $\text{KMnO}_4$  as compared to  $\text{O}_3$ . The explanation is given in the previous paragraph of section 4.2. While in the case of  $\text{KMnO}_4$  (in solid form), the oxidant is present in the reaction vessel for

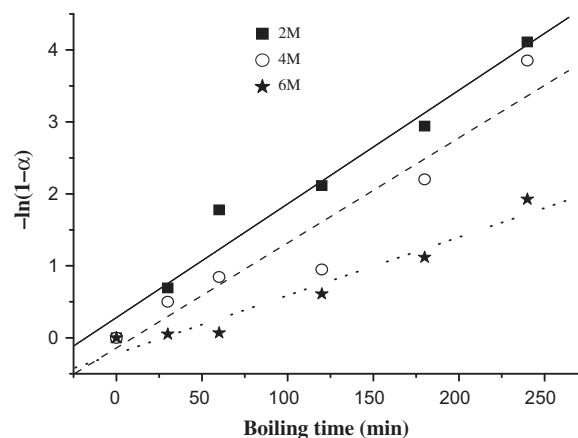


Fig. 7. Volatilisation behaviour of Ru using  $\text{KMnO}_4$  as oxidising agent, SHLLW with 2,4 and 6 M nitric acid at  $80^\circ\text{C}$ . Ru concentration 126 ppm, adsorbent PEEK, oxidant  $\text{KMnO}_4$ ,  $R = 0.98$  (2 M),  $R = 0.957$  (4 M),  $R = 0.972$  (6 M).

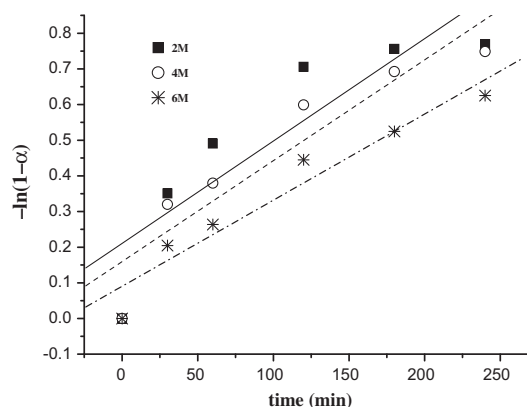


Fig. 8. Volatilisation behaviour of Ru using  $\text{O}_3$  as oxidising agent, SHLLW with 2,4 and 6 M nitric acid at  $80^\circ\text{C}$ . Ru concentration 126 ppm, adsorbent PEEK, oxidant  $\text{O}_3$  (25 g/L),  $R = 0.88$  (2 M),  $R = 0.93$  (4 M),  $R = 0.967$  (6 M).

the complete reaction time. This results in maximum oxidation of Ru ions present in the solution mixture of simulated waste. Another reason is that the electrode potential of  $\text{KMnO}_4$  is more compared to ozone. Hence,  $\text{KMnO}_4$  is able to oxidise maximum Ru present in SHLLW to  $\text{RuO}_4$ .

#### 4.7. Adsorption dynamics

It is generally acknowledged throughout the literature on physical adsorption processes that the dominant rate-controlling step is not the actual physical attachment of adsorbate to adsorbent (nor-

Table 2

Calculated values of volatilisation rate constants of SHLLW with 2, 4 and 6 nitric acid concentration, oxidants:  $\text{KMnO}_4$  and  $\text{O}_3$

Concentration of $\text{HNO}_3$ (M) in simulated waste	Volatilisation rate (K), $\text{min}^{-1}$ (for $\text{KMnO}_4$ )	Volatilisation rate (K), $\text{min}^{-1}$ (For $\text{O}_3$ )
2 M	$1.58 \times 10^{-2}$	$2.9 \times 10^{-3}$
4 M	$1.46 \times 10^{-2}$	$2.8 \times 10^{-3}$
6 M	$8 \times 10^{-3}$	$2.4 \times 10^{-3}$

mally referred to as very rapid) but rather intraparticle transport of gas within the porous structure of the adsorbent to its available surface. Interparticle transport from bulk fluid to the external surface of the porous adsorbent may also have an effect on the overall rate of adsorption under some circumstances. Transport resistances which influence the overall rate of adsorption are [13].

- (1) Mass and heat transfer of adsorbate to and from the exterior surface of the adsorbent (known as interparticle transport).
- (2) Maxwellian diffusion (bulk molecular diffusion) in moderately large pores (macropores) or Knudsen diffusion in pores (micropores) which have a diameter smaller than the mean free path of the adsorbate molecules.
- (3) Intracrystalline diffusion within the channel and cage-like structure of molecular sieve materials such as zeolites and silicalites.
- (4) Surface diffusion when adsorbate molecules move freely over the internal surface of adsorbents in parallel with intraparticle diffusion.
- (5) Heat transfer within the interior of particles occasioned by the exothermic nature of adsorption.

The relative importance of these resistances largely depends on the nature of the adsorbent and adsorbate and the conditions of temperature and pressure at which the adsorption occurs.

Adsorption kinetic data were further processed to confirm whether intraparticle diffusion is the rate limiting and to find out the rate parameter for intraparticle diffusion. Morris–Weber equation was applied to the kinetic data [14].

$$X = K_{id}(t)^{0.5} \quad (7)$$

The parameter  $K_{id}$  is the intraparticle diffusion rate constant ( $\text{mg g}^{-1} \text{min}^{-1/2}$ );  $X$  is the amount of Ru ion adsorbed per gram of adsorbent; and  $t$  is the time. In order to find out the rate-controlling step occurring

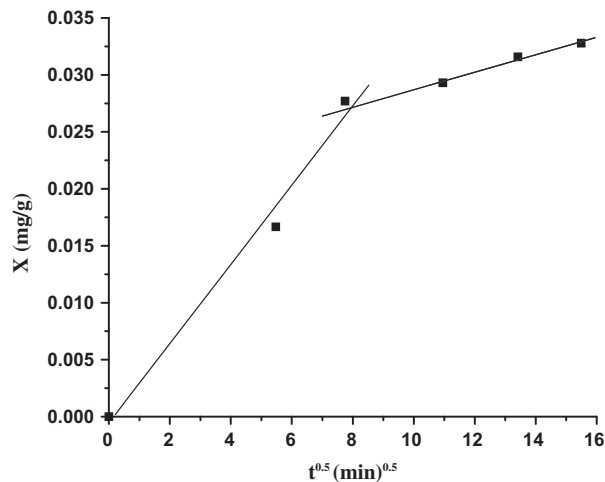


Fig. 9. Ru ions adsorbed (adsorbent: PEEK pellets, SHLLW with 2 M nitric acid concentration, Ru: 126 ppm, oxidant:  $\text{KMnO}_4$ , temperature  $80^\circ\text{C}$ ).

during adsorption, a plot of amount adsorbed at time  $t$  ( $\text{mg g}^{-1}$ ) vs.  $t^{1/2}$  was made as shown in Fig. 9 for  $\text{KMnO}_4$  and Fig. 10 for  $\text{O}_3$ .

Two distinct regions were observed; an initial linear portion is due to the boundary layer diffusion effects [15] and a second linear portion is due to the intraparticle diffusion [16]. It was also observed that the lines do not pass through the origin; indicating that there is a boundary layer resistance [17] and the magnitude of the intercepts are proportional to the extent of the boundary layer thickness [18].

In the case of  $\text{KMnO}_4$ , both intraparticle and boundary layer diffusion are playing the role of diffusion. During initial period (when  $t < 16$  min), adsorption occurs on the exterior surface of the PEEK

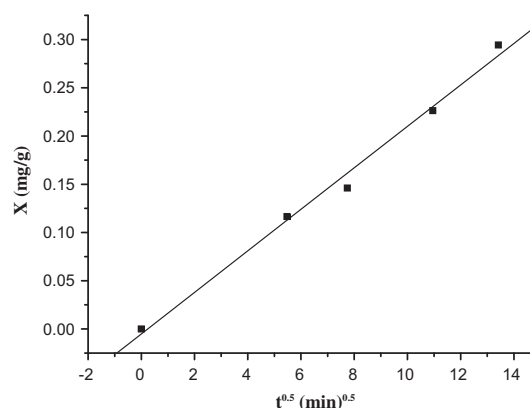


Fig. 10. Ru ions adsorbed (adsorbent: PEEK pellets, SHLLW with 2 M nitric acid concentration, Ru 126 ppm, oxidant  $\text{O}_3$  (25 g/L), temperature  $80^\circ\text{C}$ ,  $R = 0.996$ ).

pellets and correspondingly, fast adsorption rate was observed. Upon saturation of the exterior surface due to the adsorption,  $\text{RuO}_4$  diffuse into the PEEK pellets through pores and the Ru ions were absorbed by the interior surface of the particle. As a result of diffusion resistance, the intraparticle diffusion rate becomes slow.

While in the case of ozone, only boundary layer diffusion was taking place. The intraparticle diffusion and boundary layer rates for Ru ions adsorption on PEEK pellets for simulated waste with 2M nitric acid concentration were calculated and are given in Table 3.

The rate constant data indicates a higher value for ozone. Similar observation was seen during the experiments also. In the case of ozone, the blackening of PEEK pellets bed started taking place well before that of  $\text{KMnO}_4$ .

#### 4.8. Adsorption models

##### 4.8.1. Langmuir Isotherm

In order to understand the sorption behaviour, different adsorption isotherm models were employed. In this study, three isothermal equations, i.e. Langmuir, Freundlich and Dubinin–Raduskevich (D–R), are employed to study the adsorption process [9].

The isotherm is well described by the linear form of the Langmuir equation

$$\frac{C}{X} = \frac{1}{K_L X_m} + \frac{C}{X_m} \quad (8)$$

where  $C$  is the equilibrium concentration of metal ion in solution ( $\text{mg/L}$ ),  $X$  the amount of metal adsorbed at equilibrium ( $\text{mg g}^{-1}$ ),  $X_m$  the monolayer capacity ( $\text{mg g}^{-1}$ ) and  $K_L$  is the parameter of Langmuir isotherm ( $\text{L g}^{-1}$ ).

The data are not fitted well in the Langmuir isotherm as shown by the regression coefficient values  $R^2$  (Table 3), thereby indicating that the graph is deviating from linearity and curvature is observed in Fig. 11.

Table 3  
Calculated diffusion rate constants for Ru adsorption on PEEK pellet

Oxidising agent	Rate constant ( $K_{id}$ ) ( $\text{mgg}^{-1} \text{min}^{-0.5}$ )
$\text{KMnO}_4$	$K_1 = 0.00486$ $K_2 = 6.779 \times 10^{-4}$
$\text{O}_3$	0.0215

##### 4.8.2. Freundlich Isotherm

The Freundlich equation was applied to the concentration dependant data, in the linear form as Eq. (9):

$$\log X = \log K_F + \frac{1}{n} \log C \quad (9)$$

where  $X$  and  $C$  have already been defined earlier;  $n$  and  $K_F$  are the characteristic constant that can be related to the strength of the adsorptive bond. The Freundlich plot of  $\log X$  vs.  $\log C$  is shown in Fig. 12. The data fitted well in the Freundlich equation, as shown by the regression coefficient values (Table 4), which depicts the conformity of the data to the Freundlich equation in the entire concentration range studied.

The numerical values of adsorption capacity ( $K_F$ ) and intensity ( $1/n$ ) were computed from the intercepts and slopes of the straight line using least square fit program.

##### 4.8.3. D–R isotherm

The experimental equilibrium data were also analysed using D–R isotherm Eq. (10) expressed as:

$$\ln X = \ln X_m - K' \varepsilon^2 \quad (10)$$

where  $\varepsilon = RT \ln(1 + 1/C)$ ,  $K'$  is the constant related to the adsorption energy,  $R$  the gas constant and  $T$  is the temperature in Kelvin. The quantities  $X$ ,  $X_m$  and  $C$  have the same meaning as above.

The data are not well fitted in this case also. The graph is deviating from linearity and curvatures are

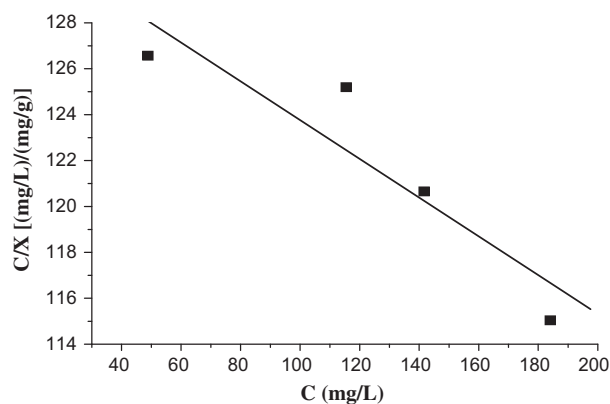


Fig. 11. Langmuir plot of Ru ions (adsorbing material: PEEK pellets, SHLLW with 4M nitric acid concentration, Ru concentration 126 ppm, oxidant:  $\text{KMnO}_4$ , temperature  $80^\circ\text{C}$ ,  $R = -0.92$ ).

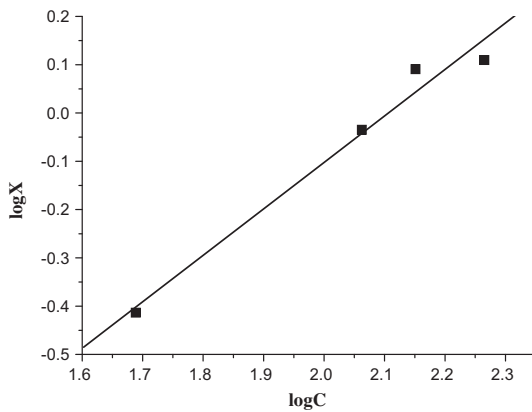


Fig. 12. Freundlich plot of Ru ions (adsorbing material: PEEK pellets, SHLLW with 4M nitric acid concentration, Ru concentration 126 ppm, oxidant:  $\text{KMnO}_4$ , temperature  $80^\circ\text{C}$ ,  $R = 0.988$ ).

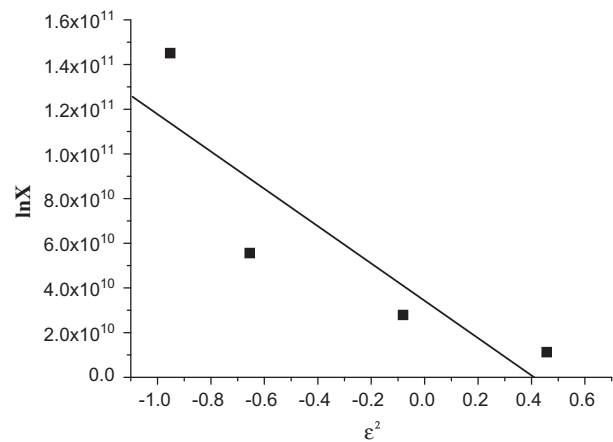


Fig. 13. D–R plot of Ru ions (adsorbing material: PEEK pellets, SHLLW with 4M nitric acid concentration, Ru concentration 126 ppm, oxidant:  $\text{KMnO}_4$ , temperature  $80^\circ\text{C}$ ,  $R = -0.87$ ).

Table 4

Calculated parameters for Ru ions adsorption on PEEK pellets from SHLLW with 4M nitric acid concentration for using  $\text{KMnO}_4$  and  $\text{O}_3$  as oxidising agent

Parameters	Values ( $\text{KMnO}_4$ as oxidising agent)	Values ( $\text{O}_3$ as oxidising agent)
Langmuir isotherm		
$X_m$ ( $\text{mgg}^{-1}$ )	-13.40	-3.377
$K_L$ ( $\text{Lg}^{-1}$ )	$-5.6793 \times 10^{-4}$	$-1.296 \times 10^{-3}$
$R^2$	0.8559	0.5167
Freundlich isotherm		
$1/n$	1.0562	1.176
$K_F$	0.006295	0.0023163
$R^2$	0.9988	0.9663
D–R isotherm		
$X_m$ ( $\text{gg}^{-1}$ )	1.46	1.93
$K$	$9 \times 10^{-12}$	$2 \times 10^{-10}$
$R^2$	0.9273	0.9929

observed. It indicates that adsorption of Ru ions on PEEK pellets also does not obey the D–R isothermal equation in the entire concentration range studied. Values of  $X_m$  and  $K'$  are calculated from the intercepts and slopes of the plot in Fig. 13.

Equilibrium concentration data for ozone as oxidising agent was also tested using the three above-mentioned adsorbent isotherms as shown in Figs. 14–16.

The concentration data generated in the case of  $\text{O}_3$  are also following the Freundlich equation, which shows physisorption.

Ru volatilisation was carried out from simulated waste using two different oxidising agent  $\text{KMnO}_4$  and  $\text{O}_3$ . The adsorption behaviour of Ru on PEEK pellets

are studied and the calculated values for all the three isotherms are given in Table 4.

It was observed that the data fitted well in the Freundlich equation for both  $\text{KMnO}_4$  and  $\text{O}_3$ , as shown by the regression coefficient values  $R^2$  (Table 4). This is an indicative of physical adsorption which is a multilayer adsorption.

#### 4.9. Thermodynamic studies

Physical adsorption is an exothermic process and heat is always released when adsorption occurs. This is always the case may be justified thermodynamically. When any spontaneous process occurs (physical adsorption of a gas at a porous surface is one such instance), there is a decrease in Gibbs free energy

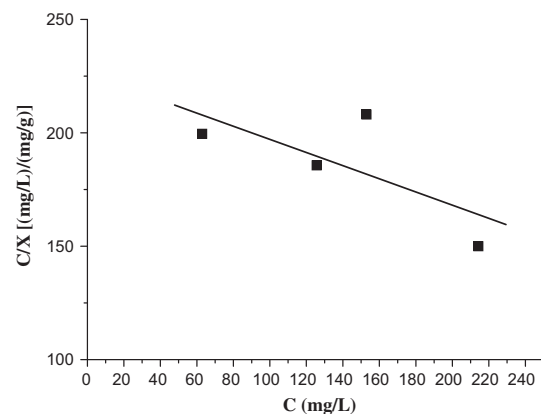


Fig. 14. Langmuir plot of Ru ions (adsorbing material: PEEK pellets, SHLLW with 4M nitric acid concentration, Ru concentration 126 ppm, oxidant:  $\text{O}_3$  (25 g/L), temperature  $80^\circ\text{C}$ ,  $R = -0.711$ ).

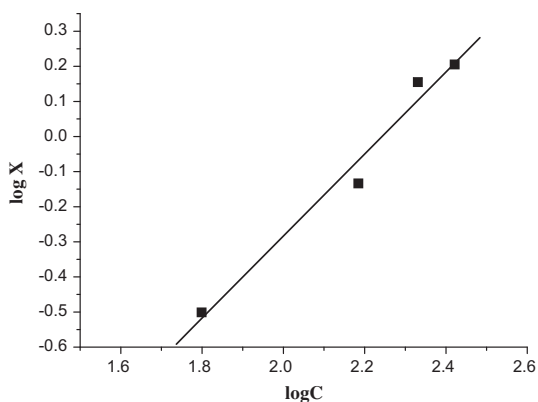


Fig. 15. Freundlich plot of Ru ions (adsorbing material: PEEK pellets, SHLLW with 4 M nitric acid concentration, Ru concentration 126 ppm, oxidant  $O_3$  (25 g/L), temperature  $80^\circ C$ ,  $R = 0.988$ ).

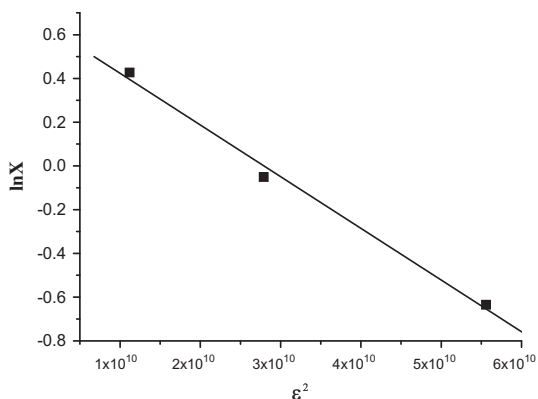


Fig. 16. D–R plot of Ru ions (adsorbing material: PEEK pellets, SHLLW with 4 M nitric acid concentration, Ru concentration 126 ppm, oxidant:  $O_3$  (25 gm/L), temperature  $80^\circ C$ ,  $R = -0.986$ ). Experimental detail: Ru concentration—126 ppm, nitric acid concentration—4 M, Adsorbent—PEEK, oxidant— $O_3$ .

( $\Delta G < 0$ ). Further, there must also be a decrease in entropy because the gaseous molecules lose at least one degree of freedom (of translation) when adsorbed. It follows then from the thermodynamic expression that  $\Delta H$  also decreases (that is, heat is released).

$$\Delta G = \Delta H - T\Delta S \quad (11)$$

Temperature is an important parameter in adsorption reactions. Adsorption usually decreases with the increase in temperature and molecules adsorbed earlier on the surface tend to desorb at elevated temperatures. However, at higher temperature, increasing molecular motion and decreasing viscosity of the solution causing the increase in adsorption have been reported in the case of activated carbon [19].

Adsorption of metal ions by solid is a kinetic process; hence, temperature may affect the adsorption process.

The influence of temperature variation was examined on the volatility and sorption of Ru on PEEK adsorbent material at temperatures 60, 70 and  $80^\circ C$ . The plot of  $\log K_c$  vs.  $1/T$  is shown in Figs. 17 and 18 for  $KMnO_4$  and  $O_3$  oxidising materials, respectively. For the value of  $K_c$ , the equilibrium constant can be worked at each temperature using the following relationship:

$$K_c = \frac{F_e}{1 - F_e} \quad (12)$$

where  $F_e$  is the fraction sorbed at equilibrium and is given by:

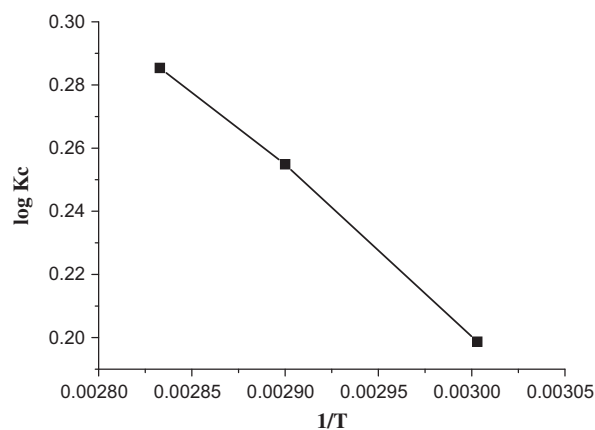


Fig. 17. Ru ions adsorption (adsorbing material PEEK pellets, SHLLW with 4 M nitric acid concentration, Ru solution concentration 126 ppm, temperature  $80^\circ C$ , oxidant:  $KMnO_4$ ,  $R = -0.998$ ).

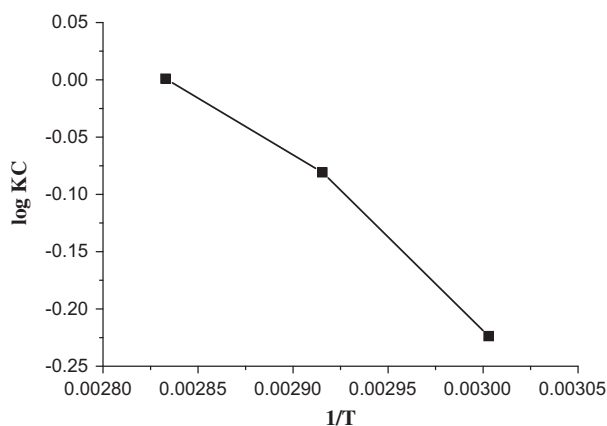


Fig. 18. Ru ions adsorption (adsorbing material PEEK pellets, SHLLW with 4 M nitric acid concentration, Ru solution concentration 126 ppm, oxidant:  $O_3$  (25 g/L), temperature  $80^\circ C$ ,  $R = -0.99$ ).

Table 5

Calculated values of thermodynamic parameters of Ru ions adsorption on PEEK pellets from SHLLW with 4M nitric acid using  $\text{KMnO}_4$  and  $\text{O}_3$  as oxidising agent

Temperature (K)	$\Delta G$ (kJ/mol)		$\Delta H$ (kJ/mol)		$\Delta S$ (kJ/mol K)	
	( $\text{KMnO}_4$ )	( $\text{O}_3$ )	( $\text{KMnO}_4$ )	( $\text{O}_3$ )	( $\text{KMnO}_4$ )	( $\text{O}_3$ )
333	-1.26	-1.46	9.745	25.34	33.06	0.07194
343	-1.53	-1.62				
353	-1.80	-2.00				

$$F_e = \frac{A_i - A_f}{A_i} \quad (13)$$

where  $A_i$  and  $A_f$  are initial and final concentrations of the adsorbing species.

The equations given below may be used to evaluate the values of  $\Delta G$ ,  $\Delta H$  and  $\Delta S$ .

$$\Delta G = -RT \ln K_c \quad (14)$$

$$\Delta G = \Delta H - T\Delta S \quad (15)$$

Combining above two equations,

$$-2.303RT \log K_c = \Delta H - T\Delta S$$

$$\log K_c = \frac{-\Delta H}{2.303RT} + \frac{\Delta S}{2.303R} \quad (16)$$

where  $\Delta H$  is the enthalpy changes for the process,  $\Delta S$  the entropy change for the process and  $G$  is the free energy change for the specific adsorption.  $R$  is gas constant (kJ/Kmol) and  $T$  is the absolute temperature (K). Values of  $\Delta H$  and  $\Delta S$  were computed from the slopes and the intercepts of linear variations of  $\log K_c$  with the reciprocal of temperature as shown in Figs. 17 and 18 for  $\text{KMnO}_4$  and  $\text{O}_3$ , respectively.

The values of  $\Delta H$  and  $\Delta S$  are given in Table 5 along with the values of  $\Delta G$  calculated from Eq. (14). The negative values of  $\Delta G$  indicate that the adsorption process is spontaneous; the positive value of  $\Delta H$  confirms the endothermic adsorption of Ru and the positive  $\Delta S$  suggests the increased randomness at the interface during the adsorption of Ru on activated PEEK material [5].

## 5. Conclusions

Preliminary experiments performed with different adsorbents showed that PEEK pellets is an effective adsorbent for removal of  $\text{RuO}_4$  from simulated high-level waste solution.  $\text{KMnO}_4$  is the best oxidising

agent compared to  $\text{O}_3$  and  $\text{K}_2\text{S}_2\text{O}_8$ . This could be due to the higher electrode potential of  $\text{KMnO}_4$ . Only 10% volatilisation was obtained for SHLLW solution without adding any oxidising agent. Volatilisation rate of Ru was found to be dependent on nitric acid concentration, Ru concentration in the solution and the temperature.

Ru volatilisation is directly dependent on temperature. When the temperature is increased from 60 to 80°C, the per cent of Ru volatilisation is increased. Adsorption of  $\text{RuO}_4$  on PEEK pellets increases with the increase in the concentration of Ru in the SHLLW solution. The observed increase is quite obvious. On increasing the concentration of Ru, more will be the concentration of  $\text{RuO}_4$  in vapour phase and more the amount gets adsorbed on PEEK pellets.

Low nitric acid concentration in SHLLW favours the volatilisation of Ru. The mechanism of adsorption of  $\text{RuO}_4$  on PEEK pellets is both intraparticle and boundary layer diffusion in the case of  $\text{KMnO}_4$ ; whereas in the case of  $\text{O}_3$ , boundary layer diffusion plays an important role.

Adsorption of  $\text{RuO}_4$  on PEEK pellets is physisorption as experimental data follows the Freundlich isotherm equation. The positive  $\Delta H$  value has indicated that the adsorption process is endothermic in nature with negative  $\Delta G$  (for spontaneous process) and positive  $\Delta S$  values.

## References

- [1] R.G. Yeotikar, M.S. Sonavane, J.G. Shah, R. Kanwar, SMART-93, pp. 257–260.
- [2] E.I. Waytt, R.R. Rickard, The Radiochemistry of Ruthenium, Oak Ridge National Laboratory, Oak Ridge, TN, 1981.
- [3] A.A. Siczek, M.J. Steindler, The chemistry of ruthenium and zirconium in the PUREX solvent extraction process, At. Energy Rev. 16 (1978) 575–618.
- [4] R. Qadeer, N. Khalid, Removal of cadmium from aqueous solutions by activated charcoal, Sep. Sci. Technol. 40 (2005) 845–859.
- [5] J. Singh, P.M. Wagh, Environmental management of Indian nuclear power plants, Int. J. Nucl. Power 16(3–4) (2002) 25–31.

- [6] S. Music, M. Ristic, Adsorption of microamounts of ruthenium on hydrous iron oxides, *J. Radioanal. Nucl. Chem.* 109 (2) (1987) 495–506.
- [7] R. Selvakumar, S. Aravindh, C.P. Kaushik, V.G. Katarani, V.S. Thorat, P. Gireesan, V. Jayavignesh, K. Swaminathan, K. Raj, Screening of silver nanoparticles containing carbonized yeast cells for adsorption of few long-lived active radionuclides, *J. Radioanal. Nucl. Chem.* 288 (2011) 629–633.
- [8] C.E. May, K.L. Rohde, B.J. Newby, B.D. Withers, Rept. OD-14439 (1958).
- [9] R. Qadeer, Adsorption behavior of ruthenium ions on activated charcoal from nitric acid medium, *Colloids Surf. A. Physicochem. Eng. Aspect* 293 (2007) 217–223.
- [10] J. Kragten, *Atlas of Metal-Ligand Equilibria in Aqueous Solutions*, Howard, Chichester, (1978), p. 781.
- [11] G.G. Eichholz, J. Hazards and control of ruthenium in the nuclear fuel cycle, *Radioanal Nucl. Chem.* 2 (1978) 29–76.
- [12] A.S. Wilson, Ruthenium volatilization in the distillation of nitric acid, *J. Chem. Eng. Data* 5 (1960) 521–524.
- [13] W.J. Thomas, B. Crittenden, *Adsorption Technology and Design*, 1 (1998) 38–42.
- [14] W.J. Weber, J.C. Morris, Intraparticle diffusion during the sorption of surfactants onto activated carbon, *J. Saint. Eng. Div. Am. Soc. Civil Eng.* 89 (1963) 53–61.
- [15] J. Crank, *The Mathematics of Diffusion*, Clarendon Press, Oxford, 1965.
- [16] G. McKay, M.S. Otterburn, A.G. Sweeney, The removal of colour from effluent using various adsorbents—III. Silica: Rate processes, *Water Res.* 14 (1980) 15–20.
- [17] M. Yalcin, A. Gurses, C. Dogar, M. Sozibilir, The adsorption kinetics of Cethyltrimethylammonium Bromide (CTAB) onto powdered active carbon, *Adsorption* 10 (2004) 339–348.
- [18] C.K. Jain, M.K. Sharma, Adsorption of cadmium on bed sediments of river Hindon: Adsorption models and kinetics, *Water Air Soil Pollut.* 137 (2002) 1–19.
- [19] M. Horsfall Jr., A.I. Spiff, Effects of temperature on the sorption of Pb<sup>2+</sup> and Cd<sup>2+</sup> from aqueous solution by *Caladium bicolor* (Wild Cocoyam) biomass, *E-J. Biotechnol.* 8 (2) (2005) 162–169.